Influence of Elbow Flexion and Stimulation Site on Neuromuscular Electrical Stimulation of the Biceps Brachii

Eric J. Gonzalez, Ryan J. Downey, Courtney A. Rouse, and Warren E. Dixon

***Abstract*— Functional electrical stimulation (FES) can help individuals with physical disabilities by assisting limb movement; however, the change in muscle geometry associated with limb movement may affect the response to stimulation. The aim of this paper was to quantify the effects of elbow flexion and stimulation site on muscle torque production. Contraction torque about the elbow was measured in 12 healthy individuals using a custom elbow flexion testbed and a transcutaneous electrode array. Stimulation was delivered to six distinct sites along the biceps brachii over 11 elbow flexion angles. Flexion angle was found to significantly influence the optimal (i.e., torque-maximizing) stimulation site ($\chi^2(10, N = 24) = 135.75, p = 3.12 \times 10^{-24}$), with post hoc analysis indicating a proximal shift in optimal stimulation site with increased flexion. Similarly, the biceps stimulation site was found to significantly influence the flexion angle at which peak torque occurred ($\chi^2(5, N = 24) = 101.82, p = 2.18 \times 10^{-20}$), with post hoc analysis indicating an increase in peak-torque flexion angle as stimulation site is moved proximally up the biceps. Since maximizing muscle force per unit stimulation is a common goal in rehabilitative FES, future efforts could examine methods which compensate for the shift in optimal stimulation site during FES-induced limb movement.**

***Index Terms*— Elbow flexion, electrode array, functional electrical stimulation (FES), neuromuscular electrical stimulation (NMES).**

I. Introduction

NEUROMUSCULAR electrical stimulation (NMES) is the application of an electrical stimulus to activate motor neurons thereby eliciting a muscle contraction. Functional electrical stimulation (FES) is the use of NMES to specifically yield functional limb motion (e.g., grasping, walking, reaching, and cycling). Both NMES and FES are often used in rehabilitative settings to increase muscle strength and function [1]–[5]. Furthermore, a common application of FES is the restoration of limb function in individuals post stroke, spinal cord injury or other neurological disorders, with the aim of improving daily function via external stimulation [6]–[10]. Traditionally, the implementation of FES involves the use of 2 surface electrodes per muscle group to deliver current and produce a desired response. It is known, however, that muscle length varies with limb flexion/extension [11], [12], and electrode position relative to the underlying muscle can impact contraction strength [13]. Since functional limb flexion and extension through a wide range of motion is desired, understanding the influence of changing muscle geometry on muscle response to stimulation may lead to improved methods of delivering FES. This is particularly true when FES is applied over the muscle belly (as opposed to the nerve trunk), which may shift with functional movement – thus, this work will focus on stimulation applied over the muscle belly.

One drawback of traditional FES (i.e., implemented with 2 typically large surface electrodes) is the overflow of stimulation to nearby muscles that do not contribute to the functional goal, resulting in unnecessary discomfort [14] and imprecise motor control in patients [15], [16]. Hence, proper electrode size and placement relative to the underlying skeletal muscle should be considered. In particular, the proximity of stimulation to muscle motor points has been shown to increase muscle force output per unit stimulation intensity while reducing patient discomfort [17]–[19], thereby yielding more efficient and comfortable limb movement. Here, the term motor point is used to describe the skin area superficial to the muscle where the motor activation threshold is minimized for a given electrical input [18]. Furthermore, it is known that increased muscle force output during NMES/FES can improve muscle strengthening [20]. Since improved muscle strength and patient comfort are common goals in rehabilitative settings, targeting optimal stimulation sites such as motor points during FES may lead to improved rehabilitative treatments.

Muscle geometry (i.e., muscle shape, length, and size) may vary considerably during dynamic, functional limb motion (e.g., reaching or lifting). Consequently, the position of a

Manuscript received May 7, 2017; revised January 8, 2018; accepted February 12, 2018. Date of publication February 19, 2018; date of current version April 6, 2018. This work was supported by the NSF Award under Grant 1161260. *(Corresponding author: Eric J. Gonzalez.)*

E. J. Gonzalez was with the University of Florida, Gainesville, FL 32611-6250 USA. He is now with the Department of Mechanical Engineering, Stanford University, Stanford, CA 94305 USA (e-mail: ejgonz@stanford.edu).

R. J. Downey was with the University of Florida, Gainesville, FL 32611-6250 USA. He is now with the College of Health Professions, Medical University of South Carolina, Charleston, SC 29425 USA (e-mail: downeyr@musc.edu).

C. A. Rouse and W. E. Dixon are with the Department of Mechanical and Aerospace Engineering, University of Florida, Gainesville, FL 32611-6250 USA (e-mail: courtneyarouse@ufl.edu; wdixon@ufl.edu).

Digital Object Identifier 10.1109/TNSRE.2018.2807762

static electrode placed on the skin may shift relative to the underlying muscle as limb motion occurs. Therefore, the aforementioned benefits of targeting precise points during FES may be enhanced by utilizing stimulation methods which increase selectivity and allow for flexibility in stimulation site.

In recent years, the use of multi-channel electrode arrays has emerged as a method to increase selectivity [21]–[23] and lower the rate of fatigue [24]–[26] during FES. Typically a one- or two-dimensional distribution of small surface electrodes, multi-channel electrode arrays are commonly used in applications requiring fine motor movement, such as grasp restoration [22], [27]–[32]. While much of the work involving multi-channel arrays has been successful for muscle contractions in stationary limbs [21], [22], [27]–[33], there has been little investigation into the use of an electrode array to maximize muscle contraction throughout the full range of motion of a limb. This is particularly significant because muscle activation using an electrode array has been suggested to depend on limb orientation and position, due to the relative shift of underlying muscle tissue beneath the skin [21].

The shape/length of the human biceps has a clear dependence on elbow flexion angle, making the biceps brachii a good candidate for the study of stimulation-induced muscle response as a function of changing muscle geometry. While some studies have explored the control of planar arm motion using closed-loop control of FES [34]–[36], the relationship between force production in the biceps, stimulation site, and upper limb orientation remains unclear. In theory, limb position information could be used to adjust the stimulation site in real-time via electrode switching, potentially leading to more efficient muscle recruitment, less fatigue, and reduced patient discomfort during FES.

The aim of this work is to examine the relationship between elbow flexion angle, stimulation site, and stimulation-induced torque production in the biceps brachii. We hypothesize that (1) the optimal (i.e., torque-maximizing) stimulation site on the biceps brachii varies with elbow flexion angle and (2) stimulation site on the biceps brachii influences the flexion angle at which peak torque occurs.

II. Methods

A. Subjects

Twelve able-bodied individuals (9 male, 3 female, ages 21–44 years) participated in the study. Written consent was obtained from all individuals prior to participation, as approved by the institutional review board at the University of Florida. Participants had no history of joint issues in the upper body and did not report any significant soreness in the biceps of either arm prior to participating in the study. Because the left and right arms of any participant may vary in strength, muscle mass, and response to stimulation, the left and right arms of each participant were considered to be distinct; thus, a total of 24 unique arms were tested in this study.

B. Apparatus and Materials

All testing was performed using the custom elbow flexion testbed depicted in Figure 1. The testbed consists of 1) a 12 VDC gear motor (Allied Motion PLA25) which governs flexion of the participant's elbow, 2) an optical encoder (US Digital HB6M) which measures the participant's elbow flexion angle, 3) a torque transducer (FUTEK TFF350) which measures the net torque about the participant's elbow axis, 4) a hinged aluminum frame to which the participant's arm is secured, and 5) a personal computer which controls flexion angle via the gear motor and collects sensor information via a data acquisition device (Quanser Q8-USB) and a compiled Simulink diagram. The arm of each participant was fit with a custom surface electrode array consisting of six self-adhesive $0.6'' \times 2.75''$ PALS® Flex-Tone electrodes (cut from an original size of $0.6'' \times 6''$) placed over the biceps and one $3'' \times 5''$ Valutrode® electrode placed over the triceps, used as the reference for each biceps electrode.[1] Stimulation to each of the six electrode subgroups (consisting of an individual biceps electrode and the shared reference electrode on the triceps) was delivered via a current-controlled 8-channel stimulator (RehaStim, Hasomed GmbH, Germany), which was controlled by a personal computer via ScienceMode (compiled as a Simulink block).

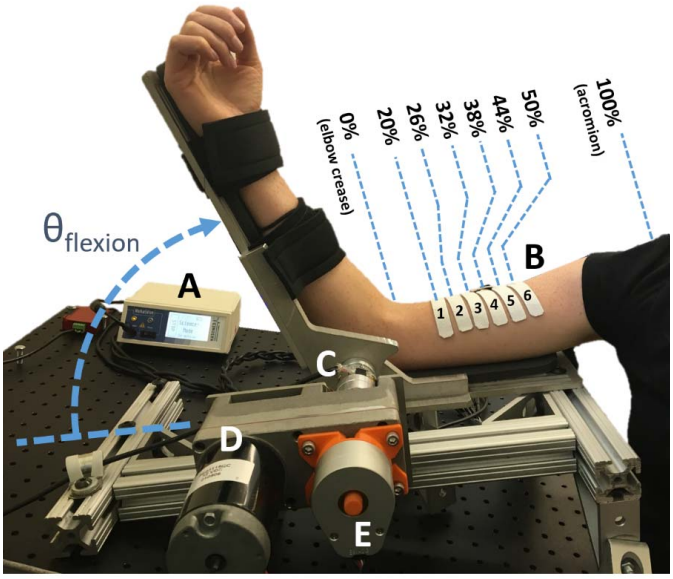

Fig. 1. The experimental setup consists of A) a current-controlled stimulator, B) an electrode array placed on the muscle belly of the participant's biceps, C) a torque transducer, D) a 12 VDC gear motor, and E) an optical encoder. Electrodes 1 through 6 and their relative locations between the elbow crease and acromion are labeled on the array above. The flexion angle of the participant's elbow is defined by θ_{flexion}. Mechanical safety limits prevent hyperflexion/hyperextension of the arm.

C. Electrode Arrangement

While the reference electrode is often positioned over the distal tendon of the biceps, in this study a large reference electrode was placed over the antagonist muscle to mirror the electrode arrangement most commonly used during muscle motor point identification [18], [37]. Each electrode subgroup

[1]Surface electrodes for the study were provided compliments of Axelgaard Manufacturing Co., Ltd.

is thus in a monopolar configuration, in which a small active electrode is used to elicit contraction of the target muscle while a large reference electrode is placed over the antagonist muscle. This configuration causes the current density of the active electrode to be greater than that of the reference electrode (as current density is inversely related to electrode area). Therefore, as the stimulation intensity is increased, motor units in proximity to the active electrode will be preferentially recruited compared to those in proximity to the reference electrode. In the present study, the reference electrode was selected sufficiently large such that a triceps contraction did not occur at the stimulation intensity tested. We note that this configuration (with reference electrode placed over the antagonist muscle) likely differs from what would be used in a functional upper-arm neuroprosthesis, as it prevents active stimulation of the triceps. Functionally, however, this configuration and that with the reference electrode placed over a tendinous area are comparable, as only tissue near the active electrode is excited [38].

Placement of the active electrode array on the biceps was standardized across participants based on the relative position of each electrode with respect to the length of the participant's upper arm. As illustrated in Figure 1, for each participant Electrode 1 was placed at 20% of the distance from the elbow crease to the acromion and Electrode 6 was placed at 50%, with the remaining electrodes spaced evenly between (i.e., a relative distance of 6% between electrodes). These relative positions were determined through preliminary experimentation and approximately cover the entire muscle belly of the biceps throughout the entire range of motion of the arm.

D. Warm-up Protocol

All participants completed a brief warm-up protocol prior to the experimental protocol to get acclimated with the sensation of NMES. During this period, each participant received 1 second of stimulation out of every 15 seconds, delivered to a single active electrode in the array. Note that the reference electrode on the triceps also received stimulation since the stimulator delivered symmetric biphasic pulses. However, the large surface area of the reference electrode ensured that current density remained below the excitation threshold and thus triceps contraction was not expected to occur. Participants indicated that they could not sense a triceps contraction, which was also confirmed by visual inspection. Additionally, participants did not report any significant skin discomfort from either the active or reference electrode during stimulation.

Stimulation was delivered at a frequency of 30 Hz with a current amplitude of 25 mA and pulse duration of 100 μs. Frequency was selected as 30 Hz since literature suggests this frequency to be a reasonable compromise between slowing fatigue and eliciting strong contractions [39]. Both pulse amplitude and duration influence the strength of elicited contractions during NMES [39]. Thus, a fixed current amplitude of 25 mA was selected based on preliminary experiments which yielded high contraction torque resolution for variation

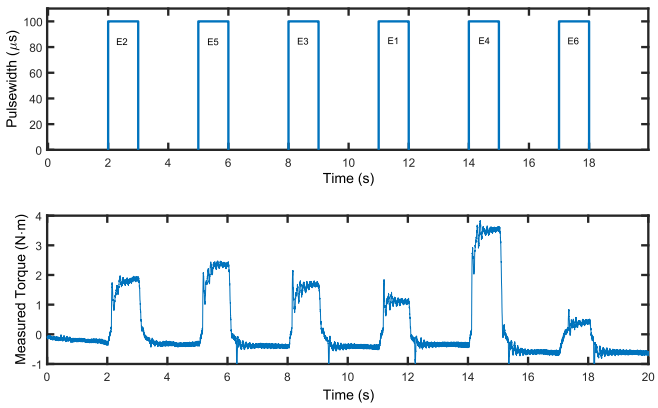

Fig. 2. Example stimulation pattern sent to the electrode array (top) and the resulting torque caused by biceps contraction (bottom) obtained from a single participant's arm fixed at a flexion angle of 90 degrees. E1 - E6 refer to Electrode 1 - Electrode 6, respectively. Note that the low frequency drift in baseline torque is accounted for when calculating mean contraction torque.

in pulse duration. A fixed pulse duration of 100 μs was then selected such that measurable torque was elicited in all person-electrode-angle combinations while not inducing contractions so strong they would cause discomfort during the experimental protocol. Since the elicited contractions were significantly less than the maximal voluntary contraction (MVC) torque based on preliminary experiments (<15%), differences in relative contraction intensity between participants were considered minimal and thus the fixed pulse duration of 100 μs was used for all participants for simplicity. The mean contraction torque elicited by these stimulation parameters at 40 degrees of flexion (i.e., the flexion angle used during warm-up) was 5.72 $\pm$ 1.99 Nm (Mean $\pm$ SD), which is approximately 10% of the reported mean biceps MVC torque for males and 15% of that reported for females according to Günzkofer et al. [40].

Prior to data collection, pulse duration was manually incremented from 20 μs to 100 μs over the course of approximately 90 seconds to familiarize the individual with the stimulation sensation. A minimum rest period of 3 minutes was required following the pretrial period prior to beginning the experimental protocol.

E. Experimental Protocol

During the experimental protocol, computer control of the motor was used to cycle the participant's arm through a randomized sequence of 11 target flexion angles (0, 10, 20, …, 100 degrees) within $\pm$ 2 degrees. At each flexion angle, each of the six biceps electrodes received 1 second of stimulation (30 Hz, 25 mA, 100 μs) in a random order as elbow torque was recorded. The motor was locked such that stimulation-induced contractions of the biceps did not alter the flexion angle of the elbow (i.e., contractions were isometric). The order of flexion angles and stimulation sites (within each flexion angle) tested were randomized to prevent systematic bias due to possible carryover effect of fatigue. An example of the stimulation pattern and induced torque measured at one fixed angle is presented in Figure 2.

F. Data Analysis

For each flexion angle and electrode combination, the mean contraction torque was calculated. Mean contraction torque (subsequently referred to simply as contraction torque) was defined as the difference between the mean torque measured during contraction (averaged from data taken in the central 0.5 seconds of the 1 second of stimulation) and the mean baseline torque measured in the 0.5 seconds prior to stimulation, during which the arm was at rest. Defining contraction torque in this way compensated for the effects of gravity and sensor drift on the measured torque. Note that the mean torque over a time window is directly proportional to the torque-time-integral over the same time window. The maximal contraction torque elicited by each arm tested was 6.58 ± 1.86 Nm (Mean $\pm$ SD), with range 6.19 Nm.

For each flexion angle in the trial an optimal electrode was determined, defined as the electrode within the array which produced the maximum mean contraction torque at that flexion angle. Similarly, for each electrode within the array, the flexion angle that yielded the maximum contraction torque was also calculated (henceforth termed the peak-torque flexion angle). In total, we stimulated the biceps and recorded contraction torque in 66 different configurations for each arm tested. Although it is certainly possible to record the torque multiple times at each configuration, the early onset of muscle fatigue is a known limitation of NMES/FES. Thus, we chose to record the torque only once at each configuration to avoid muscle fatigue as a confound.

A non-parametric Friedman test of differences was used to examine the influence of flexion angle on the optimal electrode and similarly to examine the influence of stimulation site on the peak-torque flexion angle at a significance level of 0.05. Post hoc pairwise comparisons were performed using a Wilcoxon signed rank test with a significance level of 0.05, corrected with the Bonferroni method. All statistical analysis was performed in SPSS.

III. Results

The mean normalized contraction torque for each electrode within the array (averaged across all 24 tested arms) is plotted as a function of flexion angle in Figure 3 to provide the reader with a general understanding of the relationship between stimulation site and elbow flexion angle on the resulting torque. Meanwhile, statistical analysis was performed on the distributions of observed optimal electrodes and peak-torque flexion angles, with the results subsequently described.

The distribution of peak-torque flexion angles observed for each electrode is summarized in Figure 4. A Friedman test yielded a statistically significant difference in peak-torque flexion angle dependent on stimulation site $\chi^2(5, N = 24) = 101.82$, $p = 2.18 \times 10^{-20}$. At a high level this is evidenced by Figure 4 as the data clusters about lower flexion angles for stimulation sites closer to the elbow crease (e.g., Electrode 1), and similarly about larger flexion angles for sites further from the elbow crease (e.g., Electrode 6). Post hoc analysis with Wilcoxon signed-rank tests was conducted with a Bonferroni correction applied (significance level adjusted to $p < 0.0033$),

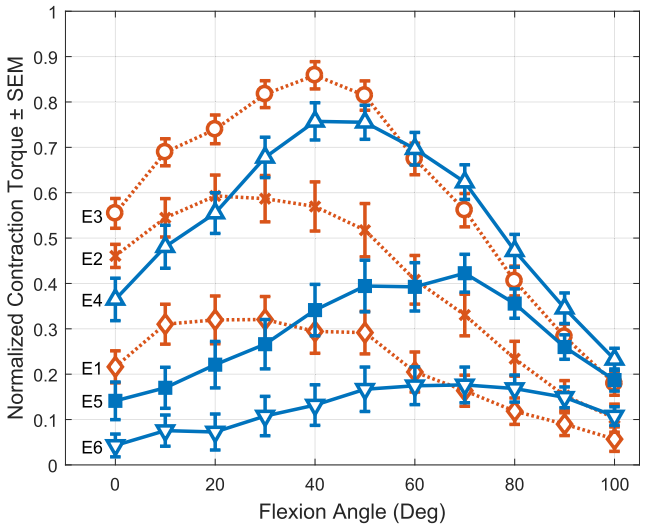

Fig. 3. Contraction torque produced by stimulation at each electrode as a function of flexion angle. To account for intersubject variability in stimulation response (i.e., contraction strength), the torque was normalized for each arm by the maximum torque elicited over the entire trial (i.e., over all 66 electrode/flexion angle combinations in the single trial). Depicted is the mean normalized contraction torque (across all 24 arms tested) $\pm$ the standard of the mean (SEM) for each data point. E1 - E6 refer to Electrode 1 - Electrode 6, respectively. Note that for each datapoint, the total number of arms tested was 24, and thus, the SD is equivalent to the SEM multiplied by a factor of sqrt(24) = 4.9.

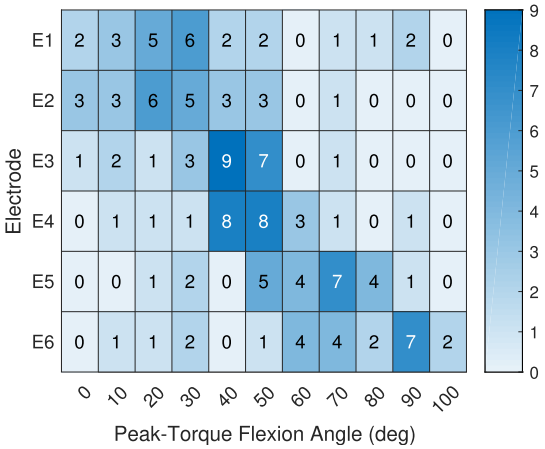

Fig. 4. Distribution of peak-torque flexion angles for each electrode position. Each row represents the distribution of peak-torque flexion angles observed for all 24 arms tested at the given electrode position. That is, each element is the number of arms yielding that peak-torque flexion angle at the given electrode position.

summarized in Table I. By this analysis, increasing electrode position (as measured proximally from the elbow) yielded a significant increase in peak-torque flexion angle in all pairwise comparisons except E3-E1 and E6-E5. This table also further depicts the general shift in median peak-torque flexion angle as stimulation shifts proximally up the biceps (from E1 to E6).

The distribution of optimal electrodes observed for each flexion angle is summarized in Figure 5. A Friedman test indicated that the optimal electrode (i.e., optimal stimulation site) varied with flexion angle $\chi^2(10, N = 24) = 135.75$, $p = 3.12 \times 10^{-24}$. At a high level this is illustrated by Figure 5,

TABLE I
PAIRWISE COMPARISON OF PEAK TORQUE FLEX. ANGLE DISTRIBUTIONS

Electrode	E1	E2	E3	E4	E5	E6
E1	M=30°	**0.003**	0.179	**0.001**	**0.000**	**0.000**
E2	**0.003**	M=25°	**0.000**	**0.000**	**0.000**	**0.000**
E3	0.179	**0.000**	M=40°	**0.000**	**0.000**	**0.000**
E4	**0.001**	**0.000**	**0.000**	M=50°	**0.000**	**0.000**
E5	**0.000**	**0.000**	**0.000**	**0.000**	M=65°	0.005
E6	**0.000**	**0.000**	**0.000**	**0.000**	0.005	M=70°

Post-hoc p-values for each electrode pair compared using a Wilcoxon signed rank test. Bold elements indicate statistically significant differences after Bonferroni correction for multiple comparisons ($p < 0.0033$). Diagonal elements list the median peak-torque flexion angle in deg. for each electrode position.

TABLE II
PAIRWISE COMPARISON OF OPTIMAL ELEC. DISTRIBUTIONS

Flex.	0°	10°	20°	30°	40°	50°	60°	70°	80°	90°	100°
0°	M=3	0.564	0.046	0.002	0.003	**0.000**	**0.000**	**0.000**	**0.000**	**0.000**	**0.000**
10°	0.564	M=3	0.083	0.003	0.005	**0.000**	**0.000**	**0.000**	**0.000**	**0.000**	**0.000**
20°	0.046	0.083	M=3	0.034	0.059	**0.000**	**0.000**	**0.000**	**0.000**	**0.000**	**0.000**
30°	0.002	0.003	0.034	M=3	0.317	0.014	0.008	**0.000**	**0.000**	**0.000**	**0.000**
40°	0.003	0.005	0.059	0.317	M=3	0.008	0.005	**0.000**	**0.000**	**0.000**	**0.000**
50°	**0.000**	**0.000**	**0.000**	0.014	0.008	M=3.5	0.564	0.025	0.014	0.014	0.034
60°	**0.000**	**0.000**	**0.000**	0.008	0.005	0.564	M=4	0.046	0.059	0.059	0.096
70°	**0.000**	**0.000**	**0.000**	**0.000**	**0.000**	0.025	0.046	M=4	0.564	0.564	0.655
80°	**0.000**	**0.000**	**0.000**	**0.000**	**0.000**	0.014	0.059	0.564	M=4	1	1
90°	**0.000**	**0.000**	**0.000**	**0.000**	**0.000**	0.014	0.059	0.564	1	M=4	1
100°	**0.000**	**0.000**	**0.000**	**0.000**	**0.000**	0.034	0.096	0.655	1	1	M=4

Post-hoc p-values for each flexion angle pair compared using a Wilcoxon signed rank test. Bold elements indicate statistically significant differences after Bonferroni correction for multiple comparisons ($p < 0.001$). Diagonal elements list the median optimal electrode for each flexion angle.

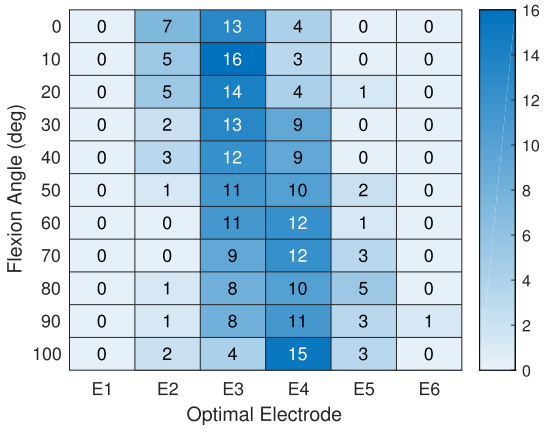

Fig. 5. Distribution of optimal electrodes for each flexion angle. Each row represents the distribution of optimal electrodes observed for all 24 arms tested at the given flexion angle. That is, each element is the number of arms yielding that optimal electrode at the given flexion angle.

which shows the concentration of observed optimal electrodes shift from Electrode 3 to Electrode 4 as flexion angle is increased. Post hoc analysis with Wilcoxon signed-rank tests was conducted with a Bonferroni correction applied (significance level adjusted to $p < 0.001$), summarized in Table II. Note that due to the large number of comparisons (55), this adjusted significance level is likely conservative. By this analysis, flexion angles 70-100 degrees yielded a significantly different optimal electrode (Median = E4) compared to flexion angles 0-40 degrees (Median = E3).

IV. DISCUSSION

The results of this study indicate that (1) flexion angle significantly influences the location of the optimal electrode within an electrode array and (2) stimulation site significantly influences the flexion angle at which contraction torque is maximal (i.e., peak-torque flexion angle). Moreover, post hoc analysis shows that increasing flexion angle leads to a statistically significant proximal shift of the optimal stimulation site, and in general shifting stimulation site up the biceps significantly increases the elbow flexion angle at which peak-torque occurs.

Figure 3 provides a visual depiction of the statistically significant trends highlighted in both Figures 4 and 5 in terms of normalized contraction torque. We see the increase in peak-torque flexion angle (in Figure 3, the flexion angle corresponding to the local maximum of each curve) as stimulation site is moved proximally up the biceps brachii (from Electrode 1 to Electrode 6). We also see that Electrode 3 tends to be optimal for lower flexion angles, and Electrode 4 for larger angles; this significant difference was statistically confirmed in post hoc analysis when comparing flexion angles 0-40 degrees with angles 70-100 degrees ($p < 0.001$). Overall 83% of all optimal electrodes observed over the entire range of motion were either Electrode 3 or 4. For flexion angles $\leq$50 degrees, Electrode 3 was optimal in 55% of observations and Electrode 4 in 27%. For flexion angles $\geq$60, Electrode 3 was optimal in 33% of observations and Electrode 4 in 50%. Along these lines, post hoc analysis (Table II) showed that flexion angles 70-100 degrees yielded a significantly different optimal electrode (Median = E4) compared to flexion angles 0-40 degrees (Median = E3).

Stimulating at these optimal locations results in the maximizing of muscle torque output per unit stimulation. Since increasing contraction intensity has been shown to improve muscle strengthening [20] and reducing stimulation is known to improve patient comfort [17], it may be beneficial to utilize an electrode array to switch between optimal stimulation sites as a function of flexion angle during NMES/FES. It should be noted, however, that while the optimal electrode was shown to depend on flexion angle, the results of this study – as evidenced by Figure 5 – indicate that variation in the optimal stimulation site was almost entirely limited between Electrodes 2 and 5 (18% of biceps length), with 83% of observed optimal electrodes being Electrodes 3 or 4 (6% of biceps length). Thus, future efforts may focus on using an array of smaller electrodes more finely distributed in this region to improve selectivity and better target the optimal stimulation site as it shifts with the underlying muscle bulk. Further investigation is needed, however, to ensure contraction torque elicited by stimulating individual, small electrodes is functional. If it turns out that the contraction torque from stimulating with smaller electrodes is not strong enough to be functional, an alternative solution

may be to use more sophisticated hardware to deliver current through multiple smaller electrodes simultaneously, thereby creating effective electrodes that have greater surface area than each individual electrode alone, while still achieving an improved spatial resolution. Along these lines, future work may compare torque elicited through stimulation of individual and combinations of electrodes within a finer resolution array placed over the optimal region, using maximal voluntary contraction as reference.

The size of this optimal region between Electrodes 3 and 4 – typically about 2 cm based on the range of elbow crease-acromion distances tested (28.5-36.8 cm) – is comparable to the results of Crochetiere et al. which found that the triceps brachii motor point linearly shifts approximately 2 cm during elbow flexion [13]. This indicates that a fine electrode array may be also a useful tool in the tracking of optimal stimulation sites of other muscles which exhibit changes in geometry during FES-induced limb flexion/extension. Although the magnitude of this shift is relatively small on the biceps brachii, Figure 3 illustrates that the mean normalized contraction torque differs by up to 20% between Electrodes 3 and 4 at smaller flexion angles. By targeting these optimal stimulation sites using selective stimulation, resulting FES for functional limb movement may result in less fatiguing, more comfortable, and more effective stimulation compared to the large electrodes conventionally used in the clinical setting. This is due to the minimization of stimulation overflow present with large conventional electrodes, which causes the contraction of muscle fibers that don't contribute to muscle torque output and can result in discomfort [14] and imprecise motor control [15], [16]. Future work may analyze the specific qualitative and quantitative neuromuscular differences of stimulation using conventional electrodes versus a targeted electrode array.

Similar to the motor point, the observed shift of the biceps optimal stimulation site mirrors that of the biceps innervation zone – the region of the biceps brachii corresponding to a high concentration of neuromuscular junctions – during elbow flexion; one previous study reported a 1.5-2 cm shift in location of the innervation zone on the biceps brachii over an 80 degree flexion range [41]. Guzmán-Venegas et al. [42] compared the locations of the innervation zone (7.6 ± 1.9 cm) and motor point (8.7 ± 1.9 cm) on the biceps brachii as measured from the distal tendon of the biceps, reporting that 30% of 20 tested subjects had the two landmarks at the same location. The close proximity and similar response to limb flexion of the motor point and innervation zone indicate the two landmarks are closely related, although the specifics of this relationship remain unclear. The innervation zone has also been shown to shift proportional to the intensity of voluntary muscle contraction [43]. Thus, it is reasonable to suggest that stimulation intensity during NMES may influence the location of the motor point (and thus, the optimal stimulation site); in particular, higher intensity stimulation may cause the muscle to shorten more, amplifying the change in muscle geometry induced by limb flexion. We note, however, that even the largest contraction-induced shift in innervation zone reported in [43] (6 ± 4 mm) is relatively small, and may be difficult to properly track. If accounting for the shift in optimal stimulation site with respect to elbow flexion proves beneficial during FES however, it may ultimately be worthwhile to account for the effects of stimulation intensity as well.

Additionally, while it is known that the elbow torque-joint angle relationship exhibits a peak [44], previous studies have not examined the effect of electrode location on the magnitude or location of this peak during NMES. The results of the present study show that electrode placement significantly influences the flexion angle at which peak torque occurs. This further emphasizes the impacts of electrode placement (i.e., stimulation site) during NMES/FES, particularly with regard to functional performance.

One limitation of the current electrode arrangement is the use of a large reference electrode on the triceps. While this mirrors experimental setups for motor point identification [18], [37], modification may be necessary for use in more general upper-arm neuroprostheses which often require active stimulation of the triceps as well. For such applications, the reference electrode for the active electrode array may be placed on the distal portion of the biceps.

V. Conclusion

The results of the present work indicate opportunities for improving functional performance during upper-arm FES applications that induce significant changes in muscle geometry (e.g., lifting or arm cycling). In particular, elbow flexion was shown to influence the optimal stimulation site within an electrode array, and stimulation site was shown to influence the flexion angle which maximizes contraction intensity during NMES. Overall, it was evidenced that muscle force output during upper-arm FES may be maximized by shifting the stimulation site with the proximal shift of the biceps brachii muscle bulk during elbow flexion. Based on these findings, future efforts could combine closed-loop control of FES with flexion angle-based electrode switching to track the muscle motor point and maximize contraction intensity throughout a desired trajectory while minimizing commanded stimulation. This may yield improved limb tracking and reduced fatigue compared to traditional NMES/FES.

References

[1] S. K. Sabut, C. Sikdar, R. Mondal, R. Kumar, and M. Mahadevappa, "Restoration of gait and motor recovery by functional electrical stimulation therapy in persons with stroke," *Disabil. Rehabil.*, vol. 32, no. 19, pp. 1594–1603, 2010.

[2] S. K. Stackhouse, S. A. Binder-Macleod, C. A. Stackhouse, J. J. McCarthy, L. A. Prosser, and S. C. K. Lee, "Neuromuscular electrical stimulation versus volitional isometric strength training in children with spastic diplegic cerebral palsy: A preliminary study," *Neurorehabil. Neural Repair*, vol. 21, no. 6, pp. 475–485, 2007.

[3] L. Snyder-Mackler, A. Delitto, S. W. Stralka, and S. L. Bailey, "Use of electrical stimulation to enhance recovery of quadriceps femoris muscle force production in patients following anterior cruciate ligament reconstruction," *Phys. Therapy*, vol. 74, no. 10, pp. 901–907, 1994.

[4] A. M. E. Scremin *et al.*, "Increasing muscle mass in spinal cord injured persons with a functional electrical stimulation exercise program," *Arch. Phys. Med. Rehabil.*, vol. 80, no. 12, pp. 1531–1536, 1999.

[5] T. Marqueste, F. Hug, P. Decherchi, and Y. Jammes, "Changes in neuromuscular function after training by functional electrical stimulation," *Muscle Nerve*, vol. 28, no. 2, pp. 181–188, 2003.

[6] T. Yan, C. W. Y. Hui-Chan, and L. S. W. Li, "Functional electrical stimulation improves motor recovery of the lower extremity and walking ability of subjects with first acute stroke," *Stroke*, vol. 36, no. 1, pp. 80–85, 2005.

[7] P. H. Peckham and J. S. Knutson, "Functional electrical stimulation for neuromuscular applications," *Annu. Rev. Biomed. Eng.*, vol. 7, pp. 327–360, Mar. 2005.

[8] J. S. Knutson, M. J. Fu, L. R. Sheffler, and J. Chae, "Neuromuscular electrical stimulation for motor restoration in hemiplegia," *Phys. Med. Rehabil. Clin. North Amer.*, vol. 26, no. 4, pp. 729–745, 2015.

[9] B. M. Doucet and L. Griffin, "Variable stimulation patterns for poststroke hemiplegia," *Muscle Nerve*, vol. 39, no. 1, pp. 54–62, 2009.

[10] V. K. Mushahwar, P. L. Jacobs, R. A. Normann, R. J. Triolo, and N. Kleitman, "New functional electrical stimulation approaches to standing and walking," *J. Neural Eng.*, vol. 4, no. 3, pp. S181–S197, 2007.

[11] T. Fukunaga, M. Ito, Y. Ichinose, S. Kuno, Y. Kawakami, and S. Fukashiro, "Tendinous movement of a human muscle during voluntary contractions determined by real-time ultrasonography," *J. Appl. Physiol.*, vol. 81, no. 3, pp. 1430–1433, 1996.

[12] A. Amis, A. Prochazka, D. Short, P. S. Trend, and A. Ward, "Relative displacements in muscle and tendon during human arm movements," *J. Physiol.*, vol. 389, no. 1, pp. 37–44, 1987.

[13] W. J. Crochetiere, L. Vodovnik, and J. B. Reswick, "Electrical stimulation of skeletal muscle—A study of muscle as an actuator," *Med. Biol. Eng.*, vol. 5, no. 2, pp. 111–125, 1967.

[14] R. J. Triolo, M. Q. Liu, R. Kobetic, and J. P. Uhlir, "Selectivity of intramuscular stimulating electrodes in the lower limbs," *J. Rehabil. Res. Develop.*, vol. 38, no. 5, pp. 533–544, 2001.

[15] R. H. Nathan, "FNS of the upper limb: Targeting the forearm muscles for surface stimulation," *Med. Biol. Eng. Comput.*, vol. 28, no. 3, pp. 249–256, 1990.

[16] A. M. Sagi-Dolev, D. Prutchi, and R. H. Nathan, "Three-dimensional current density distribution under surface stimulation electrodes," *Med. Biol. Eng. Comput.*, vol. 33, no. 3, pp. 403–408, 1995.

[17] M. Gobbo, P. Gaffurini, L. Bissolotti, F. Esposito, and C. Orizio, "Transcutaneous neuromuscular electrical stimulation: Influence of electrode positioning and stimulus amplitude settings on muscle response," *Eur. J. Appl. Physiol.*, vol. 111, no. 10, pp. 2451–2459, 2011.

[18] M. Gobbo, N. A. Maffiuletti, C. Orizio, and M. A. Minetto, "Muscle motor point identification is essential for optimizing neuromuscular electrical stimulation use," *J. Neuroeng. Rehabil.*, vol. 11, no. 1, p. 17, 2014.

[19] B. J. Forrester and J. S. Petrofsky, "Effect of electrode size, shape, and placement during electrical stimulation," *J. Appl. Res.*, vol. 4, no. 2, pp. 346–354, 2004.

[20] H. S. Lai, G. D. Domenico, and G. R. Strauss, "The effect of different electro-motor stimulation training intensities on strength improvement," *Aust. J. Physiother.*, vol. 34, no. 3, pp. 151–164, 1988.

[21] D. B. Popović and M. B. Popović, "Automatic determination of the optimal shape of a surface electrode: Selective stimulation," *J. Neurosci. Methods*, vol. 178, no. 1, pp. 174–181, Mar. 2009.

[22] T. Keller, M. Lawrence, A. Kuhn, and M. Morari, "New multichannel transcutaneous electrical stimulation technology for rehabilitation," in *Proc. Conf. IEEE Eng. Med. Biol. Soc.*, Aug./Sep. 2006, pp. 194–197.

[23] J. P. Dmochowski, A. Datta, M. Bikson, Y. Su, and L. C. Parra, "Optimized multi-electrode stimulation increases focality and intensity at target," *J. Neural Eng.*, vol. 8, no. 4, p. 046011, 2011.

[24] N. M. Malešević, L. Z. Popović, L. Schwirtlich, and D. B. Popović, "Distributed low-frequency functional electrical stimulation delays muscle fatigue compared to conventional stimulation," *Muscle Nerve*, vol. 42, no. 4, pp. 556–562, 2010.

[25] R. J. Downey, M. J. Bellman, H. Kawai, C. M. Gregory, and W. E. Dixon, "Comparing the induced muscle fatigue between asynchronous and synchronous electrical stimulation in able-bodied and spinal cord injured populations," *IEEE Trans. Neural Syst. Rehabil. Eng.*, vol. 23, no. 6, pp. 964–972, Nov. 2015.

[26] R. J. Downey, T.-H. Cheng, M. J. Bellman, and W. E. Dixon, "Closed-loop asynchronous neuromuscular electrical stimulation prolongs functional movements in the lower body," *IEEE Trans. Neural Syst. Rehabil. Eng.*, vol. 23, no. 6, pp. 1117–1127, Nov. 2015.

[27] N. Malešević, L. Z. Popović, G. Bijelić, and G. Kvaščev, "Muscle twitch responses for shaping the multi-pad electrode for functional electrical stimulation," *J. Autom. Control*, vol. 20, no. 1, pp. 53–58, 2010.

[28] U. Hoffmann, M. Deinhofer, and T. Keller, "Automatic determination of parameters for multipad functional electrical stimulation: Application to hand opening and closing," in *Proc. IEEE Eng. Med. Biol. Soc.*, Aug. 2012, pp. 1859–1863.

[29] L. Popović-Maneski *et al/*, "Multi-pad electrode for effective grasping: Design," *IEEE Trans. Neural Syst. Rehabil. Eng.*, vol. 21, no. 4, pp. 648–654, Jul. 2013.

[30] N. Malešević *et al.*, "A multi-pad electrode based functional electrical stimulation system for restoration of grasp," *J. Neuroeng. Rehabil.*, vol. 9, no. 1, p. 66, 2012.

[31] O. Schill, R. Rupp, C. Pylatiuk, S. Schulz, and M. Reischl, "Automatic adaptation of a self-adhesive multi-electrode array for active wrist joint stabilization in tetraplegic SCI individuals," in *Proc. IEEE Toronto Int. Conf.*, Sep. 2009, pp. 708–713.

[32] T. A. Excell, C. T. Freeman, K. L. Meadmore, A.-M. Hughes, E. Hallewell, and J. Burridge, "Optimisation of hand posture stimulation using an electrode array and iterative learning control," *J. Autom. Control*, vol. 21, no. 1, pp. 1–4, 2013.

[33] A. Elsaify, "A self-optimising portable fes system using an electrode array and movement sensors," Ph.D. dissertation, Dept. Eng., Univ. Leicester, Leicester, U.K., May 2005.

[34] A. M. Hughes *et al.*, "Feasibility of iterative learning control mediated by functional electrical stimulation for reaching after stroke," *Neurorehabilitation Neural Repair*, vol. 23, no. 6, pp. 559–568, 2009.

[35] H. Dou, K. K. Tan, T. H. Lee, and Z. Zhou, "Iterative learning feedback control of human limbs via functional electrical stimulation," *Control Eng. Pract.*, vol. 7, no. 3, pp. 315–325, 1999.

[36] M. Kutlu, C. T. Freeman, E. Hallewell, A.-M. Hughes, and D. S. Laila, "Upper-limb stroke rehabilitation using electrode-array based functional electrical stimulation with sensing and control innovations," *Med. Eng. Phys.*, vol. 38, no. 4, pp. 366–379, 2016.

[37] A. Botter, G. Oprandi, F. Lanfranco, S. Allasia, N. A. Maffiuletti, and M. A. Minetto, "Atlas of the muscle motor points for the lower limb: Implications for electrical stimulation procedures and electrode positioning," *Eur. J. Appl. Physiol.*, vol. 111, no. 10, pp. 2461–2471, 2011.

[38] R. Merletti, M. Knaflitz, C. J. DeLuca, "Electrically evoked myoelectric signals," *Crit Rev Biomed Eng*, vol. 19, no. 4, pp. 293–340, 1992.

[39] B. M. Doucet, A. Lam, and L. Griffin, "Neuromuscular electrical stimulation for skeletal muscle function," *Yale J. Biol. Med.*, vol. 85, no. 2, pp. 201–215, 2012.

[40] F. Günzkofer, F. Engstler, H. Bubb, and K. Bengler, "Isometric elbow flexion and extension joint torque measurements considering biomechanical aspects," in *Proc. 1st Int. Symp. Digit. Hum. Modeling*, 2011, pp. 14–15.

[41] S. Martin and D. MacIsaac, "Innervation zone shift with changes in joint angle in the brachial biceps," *J. Electromyogr. Kinesiol.*, vol. 16, no. 2, pp. 144–148, 2006.

[42] R. A. Guzmán-Venegas, O. F. Araneda, and R. A. Silvestre, "Differences between motor point and innervation zone locations in the biceps brachii. An exploratory consideration for the treatment of spasticity with botulinum toxin," *J. Electromyogr. Kinesiol.*, vol. 24, no. 6, pp. 923–927, 2014.

[43] H. Piitulainen, T. Rantalainen, V. Linnamo, P. Komi, and J. Avela, "Innervation zone shift at different levels of isometric contraction in the biceps brachii muscle," *J. Electromyogr. Kinesiol.*, vol. 19, no. 4, pp. 667–675, 2009.

[44] Z. Hasan and R. M. Enoka, "Isometric torque-angle relationship and movement-related activity of human elbow flexors: Implications for the equilibrium-point hypothesis," *Exp. Brain Res.*, vol. 59, no. 3, pp. 441–450, 1985.